ASIAN JOURNAL OF CIVIL ENGINEERING (BUILDING AND HOUSING) VOL. 6, NO. 5 (2005)
PAGES 409-421

EXPERIMENTAL AND ANALYTICAL STUDY ON RC DEEP BEAMS

M.R. Salamy*, H. Kobayashi and Sh. Unjoh
Public Works Research Institute,
Earthquake Engineering Research Team, Minamihara 1-6, Tsukuba, Japan 305-8516

ABSTRACT

A study on RC deep beams behavior is conducted in this paper by means of finite element analysis along with experimental evaluation of analytical simulation. The beams have shear span to depth ratio between 0.5 and 1.5 and effective depth from 400 mm to 1400 mm. Lateral reinforcement ratio varies by 0.0%, 0.4% and 0.8% in shear span. A fracture type analysis is employed to simulate RC members through smeared rotating crack approach. The results showed reliability of analysis in predicting deep beams behavior in terms of failure load, failure mode as well as crack propagation. The objective of this study is to investigate capabilities of the finite element simulation for further study on deep beam behavior instead of conducting expensive time consuming experimental works. This includes particularly members with possibilities of failing in shear as well as size effect by means of large-scale structures numerical simulation.

Keywords: RC deep beam, shear failure, shear span, fracture energy, finite element

1. INTRODUCTION

The objective of this study is to investigate behavior of underground structures such as box culverts subjected to up filled materials weight as well as seismic excitation. Those structures can be modeled through a uni-span or multi-span RC frames to simplified analytical process for practical purpose. Due to heavy weight above these structures as well as lateral load components, usually the section of resisting members violate conventional size limitation for section analytical simplification such as plane section in beams under bending and shear. It is however found that such members are likely much closer to deep beam classification than any other types of members. In this regard Public Works Research Institute (PWRI) based in Tsukuba city, Kyushu Institute of Technology (KIT) and Hanshin Expressway Public Corporation (HEPC) based in Kobe city have performed sets of experiments to investigate RC deep beams behavior and lateral reinforcement effects on improving shear behavior of those beams during the year 2003 and 2004. Three sets of specimens comprise of nineteen RC

* Email-address of the corresponding author: salamy55@pwri.go.jp

beams including the experiments carried out on a joint research basis with are investigated in this study. The beams have shear span to depth ratio between 0.5 and 1.5 and effective depth size from 400 mm to 1400 mm. The longitudinal tensile reinforcement ratio is kept almost constant in about 2% for all specimens while lateral reinforcement (stirrups) ratio varies by 0.0%, 0.4% and 0.8% in shear span. The results of experiment are used to evaluate the results of finite element simulation. In order to trace compressive force path in RC beams, numbers of acrylic bars are located in between loading plates and supports to measure strain in concrete in the designated path. The objective of using this method in experiment is to verify the validation of strut-tie model and also characterize and measure actual strain in the location with highest possibility of crushing or cracking in any kind of shear failure occurs in RC beams with low a/d ratio. The results presented in this paper are part of a larger study on shear behavior of RC deep beams including size effect experimentally and numerically. A codified study on foregoing experiment is presented in [1], and therefore only a part of analytical results will be presented and discussed here.

The study of size effect on the shear strength of RC beams, which is another objective of the current study, has yet been suffering from lack of experimental evidences particularly very large-scale specimens. It is however a sound theoretical background established particularly for nonlinear size effect in fracture types material such as concrete and rock. The specimens in this study cover a wide range of size but performing test on very big specimens still is a big challenge and both time and cost consuming task for researchers. In this regard validity of finite element in prediction of RC beams behavior is examined to extend to an analytical simulation of large-scale specimens rather than conducting real experiment. Detail of analytical models is explained in further sections.

2. SPECIMENS DETAILS

Experiments carried out at PWRI and Kyushu Institute of Technology comprise nineteen RC beams with geometric characteristic and material properties given in Figure 1, Table 1 and Table 2. In Table 1, p_w, p_s, f_y, A_{st} and A_{sc} are shear span, stirrups ratio, longitudinal tensile reinforcement ratio and their yield stress, cross section area of tensile and compressive reinforcement respectively. All specimens, with or without stirrups in shear span, have a minimum lateral reinforcement in mid-span and out of span. Despite absence of shear stress in this part, which in the first look implies un-necessities of shear reinforcement, they may delay or in some case prevent the propagation of diagonal crack to compression zone. It is believed even that reinforcements in mid-span sometimes are more effective than those in shear span due to the reason stated above [2]. Since all specimens tested here have a minimum amount of stirrups at mid-span, it is however not possible to investigate lateral reinforcement effect located in that region.

Therefore, further study is necessary to confirm the effect of mid-span stirrups experimentally. In Table 2, b is specimen width, a/d and f'_c are shear span to depth ratio and compressive stress respectively. Maximum load capacity and related deflection as well as shear crack initiation load and maximum deflection are noted as P_{max}, P_{cr}^{sh}, δ_{peak} and δ_{max} respectively. Other geometrical parameters of Table 2 are schematically determined in Figure 1. All

specimens are subjected to four points monotonic static load condition. Experimental data acquisition is mainly focused on mode of failure; crack patterns, load-displacement relationship as well as steel and concrete strain in some designated locations to evaluate analytical results.

Table 1. Steel Properties of specimens

Beam	ρ_w %	ρ_{st} %	f_y Mpa	A_{st} A_{sc}	Stirrups
B-2	0.0				
B-3	0.4				D6@65
B-4	0.8				D10@75
B-6	0.0				
B-7	0.4			5D22	D6@65
B-8	0.8	2.02	376		D10@75
B-10-1	0.0			2D10	
B-10-2					
B-11	0.4				D6@65
B-12	0.8				D10@75
B-10.3-1	0.0	2.11	388	9D25 2D16	
B-10.3-2			371.7		
B-13-1	0.0	2.07	398	10D32 2D13	
B-13-2					
B-14	0.0	2.04	398	14D32 4D13	
B-17	0.4				D13@100
B-15	0.0	1.99	402	18D35 2D13	
B-16	0.0	2.05	394	18D41 2D13	D16@120
B-18	0.4		397.5		

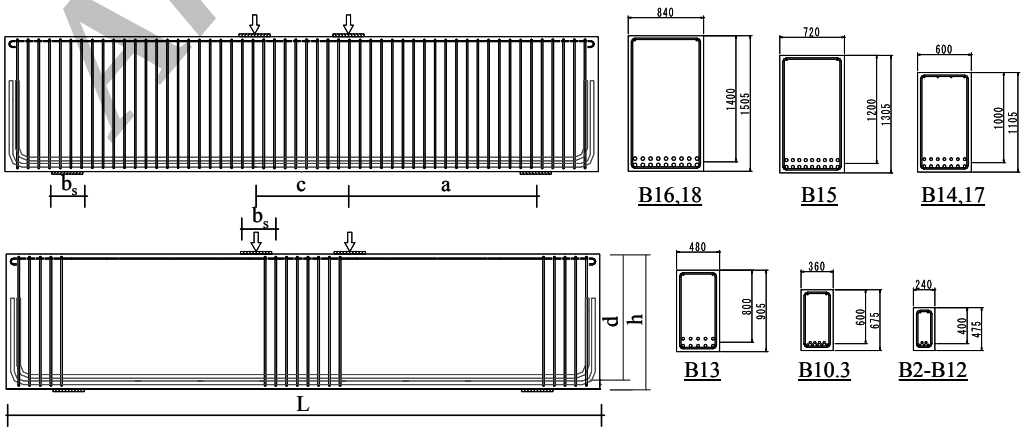

Figure 1. Detail of specimens with and without stirrups (unit: mm)

Table 2. Geometric and material properties of the specimens

Beam	a/d	Geometry size (mm)							f'_c	P_{max}	P_{cr}^{sh}	δ_{peak}	Failure Mode
		L	c	a	d	h	b	b_s	MPa	KN		(mm)	
B-2	0.5	1100	300	200	400	475	240	100	36.2	1550	525	3.16	II
B-3										1536	625	4.78	II
B-4	1.0	1500		400					31.3	1951	700	1.85	II
B-6									31.3	1050	400	2.77	II
B-7										1181	400	2.83	II
B-8									37.8	1501	600	3.26	II
B-10-1	1.5	1900	450	600	600	675	360	150	29.2	616	325	3.82	II
B-10-2									23	703	278	5.28	II
B-11									29.2	1025	350	15.96	II
B-12									31.3	1161	300	7.05	II
B-10.3-1		2850		900					37.8	1960	700	6.62	II
B-10.3-2									31.15	1787	527	8.62	II
B-13-1		3800	600	1200	800	905	480	200	31.63	2985	500	11.87	II
B-13-2									24	2257	807	9.33	II
B-14		4750	750	1500	1000	1105	600	250	31	3969	1100	9.27	II
B-17									28.7	5214	1600	11.92	II
B-15		5700	900	1800	1200	1305	720	300	27	5390	1500	11.91	II
B-16		6650	1050	2100	1400	1505	840	350	27.3	5975	1900	10.57	II
B-18									23.5	8396	2400	15.79	II

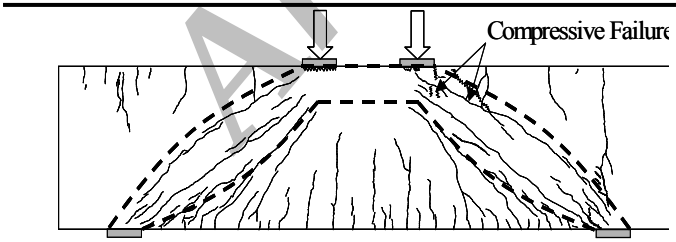

Figure 2. Crack pattern of beam 18

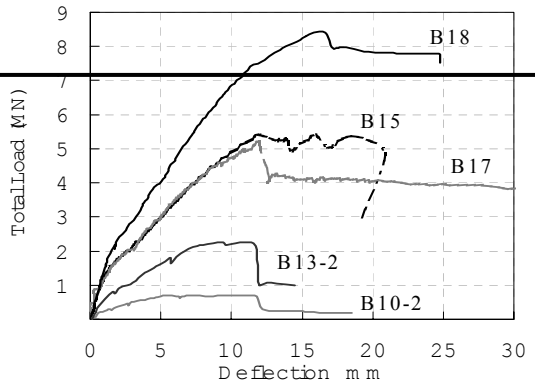

Figure 3. Load reserve after peak

3. SHEAR FAILURE MECHANISM OF RC BEAMS

Failure modes are so determined in two main categories of flexural failure mode (Mode I) and shear failure mode (Mode II) with three subcategories for Mode II failure as followings:

Mode II-1: Diagonal tension failure, which in the line of thrust become so eccentric and give rise to flexural failure in compressive zone. It is important however to mention that this kind of failure is a result of tensile crack extension in compressive zone due to the flexural load.

Mode II-2: Shear compression failure where RC beam fails due to the development of diagonal crack into the compressive zone and reduces the area of resisting region excessively and beam crushes once generated compressive stress exceed compressive strength of concrete.

Mode II-3: Shear proper or compressive failure of struts, which is often observed in beams with very small shear span to depth ratio a/d (about a/d<1.5). In this case due to the small a/d ratio, the line of thrust will be so steep and arch action not only reserve flexural capacity in most cases but also efficiently sustains required shear force. Arch formation is clearly observed in those beams and finally beams fail due to either sudden tensile crack formation parallel to the strut axes or compressive crush in normal direction to the strut axes. The latter case shows more reserved load after crushing (for instance Beams 13, 10.3 and B18). Figure 2 depicts crack pattern of B-18 at the last stage of loading where the beam failed as a result of strut compressive failure in the location stated in the Figure. Thrust zone is schematically shown in this Figure. Despite compressive failure in strut the beam sustained almost 80% of peak load and a plateau formed after a small drop in load-displacement curve. This phenomenon happened in some other beams such as B17 and B15, which is in contrary to what shear failure naturally implies as a sudden failure. Some results for specimens with large reserving load capacity after peak load are shown in Figure 3. Note however that concrete is a rate dependent material so loading rate is supposed to have considerable effect on RC member behaviors and should be taken into account properly in numerical simulation.

It is also worth to note that arch action requires a substantial horizontal reaction at the support to be formed. To satisfy this condition main bars in all specimens are well anchored with a rather long hook beyond support region. In this study only the effect of shear span stirrups have been considered though it would be of interest to study on stirrups in mid-span in preventing diagonal crack extension to compressive zone for larger a/d ratios as stated above.

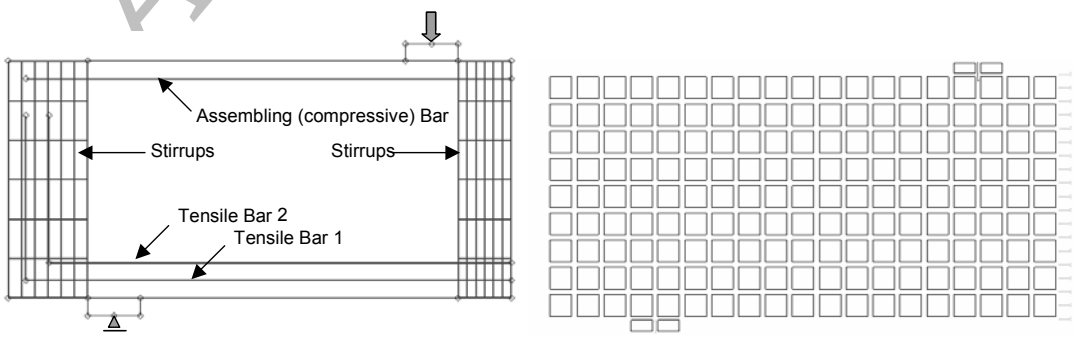

Figure 4. Analytical model and FE mesh discretization (shrink mesh)

4. FINITE ELEMENT SIMULATION

In order to conduct parametric study on a larger number of RC beams with different geometry, reinforcement and material parameters, a nonlinear finite element analysis by means of a general FE code (DIANA 8.1.2) is applied here with material models explained hence after. The constitutive behavior of concrete is represented by a smeared crack model, which in the damaged material still continuum. Analytical scheme and finite element mesh discretization is shown in Figure 4. For specimens with stirrups in shear span, lateral reinforcement will be extended to entire length of the member. According to concrete crack model, two approaches can be highlighted as fixed crack and rotating crack theory.

In the fixed crack model, once crack initiates in a finite element, the crack direction is calculated according to the principal stress direction. The crack direction is kept constant during further load increments and considered as the material axis of orthotropy. As a general case, principal stress directions need not to be coincide with axes of orthotropy and can rotate during loading process. This assumption produces a shear stress in crack surface. In order to prevent the effects of this artificially existed shear stress in the analysis, a shear retention factor as a reduction coefficient is always applied in this model. This factor can be either of a constant coefficient or varies during analysis as a function of crack width. Complication of this model manifests itself in definition of this parameter particularly when a constant value is assigned for entire analytical procedure. It is however important to mention here that despite flexural failure with minor affect of this parameter [3], analytical prediction of shear failure is significantly affected by this factor.

Alternatively, rotating crack model is presented where the direction of the principal stress coincides to the direction of the principal strain. Since crack direction rotates according to the principal stress direction, no shear stress is generated on the crack surface and just two principal components need to be defined. A considerable point in these two models is that in actuality, the angle of inclination of the concrete struts at failure usually lies between calculated angles through the fixed crack model and the rotating crack model. Therefore, these two theories furnish the two boundaries for the true situation [4]. However to prevent consequent effect of shear retention factor definition in analysis, only the rotating crack approach is adopted in the present study. In the analyses, perfect bond is assumed for both smeared reinforcements and embedded bar reinforcements.

Displacement control with Newton-Raphson solution technique is adopted here to solve equilibrium equations along with Arc-length method to investigate possibility of snap-back instabilities, which sometimes occurs in shear failure analysis. Specimens are partly modeled by FEM due to the symmetric geometry and subjected to the proportional monotonic loads with 2D elements in plane-stress condition. According to constitutive model of concrete in tension, it is supposed that softening branch of cracked concrete is sufficient to explain tension-stiffening phenomenon therefore no additional stress due to this phenomenon is included in calculation. Steel reinforcements are modeled as an elastic

perfect plastic material with no hardening after yield point.

5. CONCRETE MODELS

Concrete constitutive models are assumed in a fracture type material framework with a characteristic length parameter to eliminate mesh size effect. Consequently the fracture energy in either tension or compression will be constant for a certain material as a function of material properties rather than specimen's geometry. This assumption accomplishes a mesh objective analysis particularly by taking into account energy released in fracture process irrelevant to the mesh discretization. The foregoing length parameter h (Figures.5 and 6) is a function of element size and estimated by $\sqrt{A}$ where A is element area.

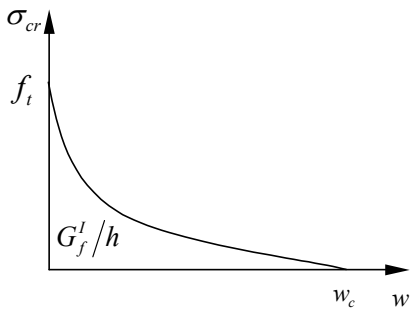

Figure 5. Concrete model in tension

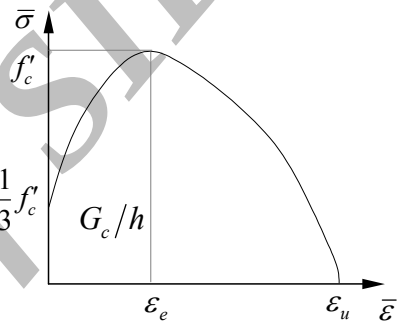

Figure 6. Concrete model in compression

5.1 Concrete in tension

Concrete in tension is modeled by constitutive model suggested by Hordijk [5] with a constant value of fracture energy shown in Figure.5. Concrete in tension before cracking is assumed to be linear elastic. After cracking however, a softening branch forms and it is assumed that the descending path follows an exponential function of crack width derived experimentally by Hordijk (1991) in Equation 1.

$$\frac{\sigma}{f_t} = \left\{1 + \left(c_1 \frac{w}{w_c}\right)^3\right\} \exp\left(-c_2 \frac{w}{w_c}\right) - \frac{w}{w_c}\left(1 + c_1^3\right)\exp\left(-c_2\right) \tag{1}$$

where w is the crack opening; w_c is the crack opening at the complete release of stress which is a function of fracture energy G_f defined by Equation 2; and σ is the normal stress in crack and f_t is the tensile strength of concrete in one dimension system or effective tensile strength in two dimension system. Values of the constants are, c_1=3, c_2=6.93.

$$w_c = 5.14 \frac{G_f}{f_t} \tag{2}$$

Tensile strength of concrete (for those specimens with no test results) and also tensile fracture energy G_f, Japan Society for Civil Engineers (JCSE design code) [6] recommendations (Eqs.3 and 4) are applied.

$$f_t = 0.23 f_c'^{\frac{2}{3}} \quad (\text{MPa}) \tag{3}$$

$$G_f = 10(d_{max})^{1/3}.f_c'^{1/3} \tag{4}$$

where d_{max} is maximum aggregate size in mm (20mm here) and G_F is fracture energy in N/m.

5.2 Concrete in compression

Concrete in compression is supposed to follow a parabolic rout that has been modified by Feenstra [7] to take into account fracture energy of concrete (Figure.6). Following equations are representing this model, which in equivalent stress is determined in terms of equivalent strain.

$$\bar{\sigma} = \begin{cases} \frac{f_c'}{3}(1 + 4\frac{\bar{\varepsilon}}{\varepsilon_e} - 2\frac{\bar{\varepsilon}^2}{\varepsilon_e^2}) & \text{if } \bar{\varepsilon} < \varepsilon_e \\ f_c'(1 - (\frac{\bar{\varepsilon} - \varepsilon_e}{\varepsilon_u - \varepsilon_e})^2) & \text{if } \varepsilon_e \le \bar{\varepsilon} < \varepsilon_u \end{cases} \tag{4}$$

$$\varepsilon_e = \frac{4}{3}\frac{f_c'}{E_c} \tag{5}$$

Consequent to the length parameter association, ultimate strain will be a function of compressive fracture energy, length parameter *h*, f_c' and also ε_e as below.

$$\varepsilon_u = 1.5\frac{G_c}{h f_c'} - \frac{11}{48}\varepsilon_e \tag{6}$$

Through this model concrete is assumed to be linear elastic up to $\frac{1}{3}f_c'$ therefore pre-peak energy will be taken into account by a correction factor $\frac{11}{48}\varepsilon_e$ in equation 6. Constant value for G_c=50 N/mm is adopted in analyses all through. Furthermore, the concept of Modified Compression Field Theory [8] is associated in analyses by means of concrete compressive strength softening due to the lateral tensile cracks.

6. COMPARISON OF THE RESULTS

Analytical predictions are compared to experiment in this section. Since all beams failed in shear (Mode II) experimentally and analytically, further results are presented based on a/d ratio in tow man categories as follows.

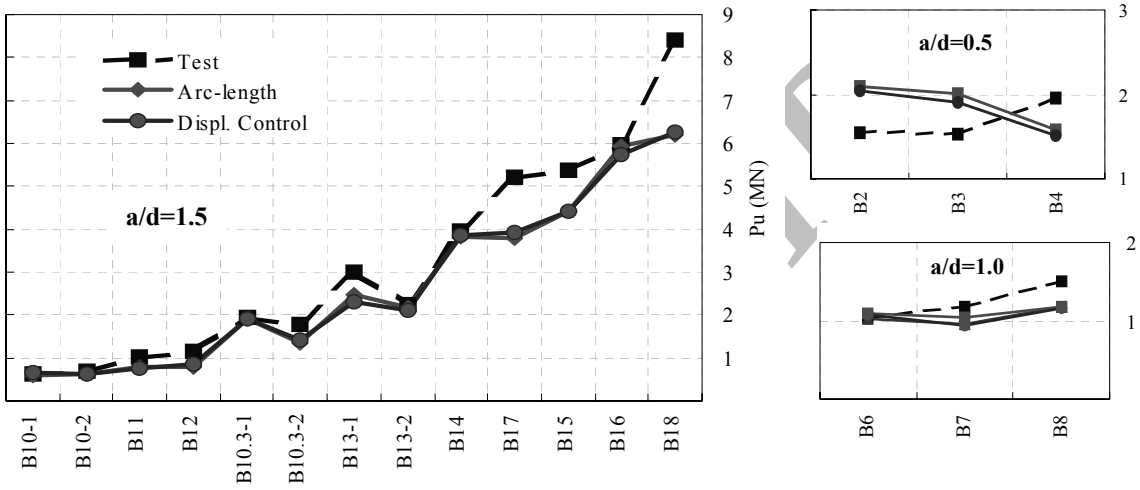

Figure 7. Beams experimental and analytical ultimate load (MN)

6.1 Load capacity

Figure 7 shows ultimate loads of specimens along with finite element prediction by conventional displacement method and Arc-length scheme. The results of two solution schemes have almost identical responses except for B16 which conventional displacement control procedure had better perdition. The results show acceptable as well as consistent numerical prediction for beams with a/d > 0.5, which in most of the modeled specimens have smaller load capacities than experiment. According to this conclusion, a safety margin for further calculation is a possible assumption, which guarantees applicability of the results. In contrary, for a/d=0.5, at least two specimens B2 and B3, analyses have predicted higher load capacity with extremely lower displacement than the experiment. In such cases if the ductility is main issue of performing analysis, the method should be however enriched with more realistic mechanism. To this end, it is supposed that for beams with very low a/d ratio, sliding bond model as well as employing an interface element between supporting plate and concrete body will correct analytical response to a certain level. The latter will eliminate undesired steel plate stiffness contribution to the entire structure stiffness matrix and also eliminates stress concentration in adjacent elements. These phenomena will be considered in the future works.

Figure 8 illustrates distribution of specimen analytical response in terms of experiment results. Dotted lines represent 15% deviation from experiment ultimate loads, which in total

FE results fall in safer zone with some exceptions of B2 and B3. Figure 9 shows analysis ultimate load to experiment for displacement control procedure. Averaged precision of analysis for with and without including specimens for beams with a/d=0.5 are 0.9 (0.91 for Arc-length) and 0.86 (0.86) respectively. This figure along with Figures.7 and 9 implies that acceptable and safe analytical results for deep beams at least for a/d >1 are obtained. Dotted lines in Figure 8 indicate 15% deviation from experiment peak loads.

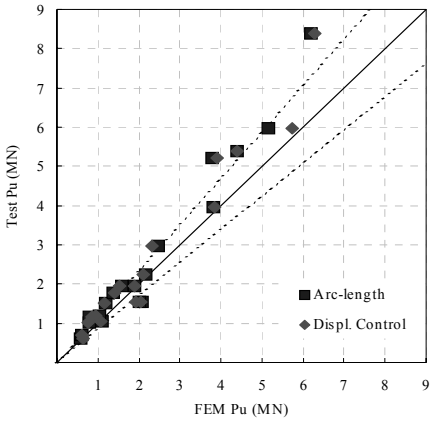

Figure 8. Analysis versus experiment

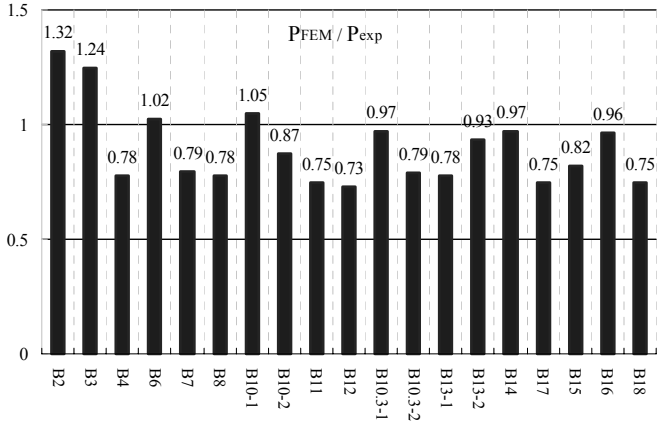

Figure 9. Analytical P_{max} to Experiment ratio

Experiment showed that shear crack initiated at about 40% of the ultimate load and full shear crack will be formed approximately in $0.5P_u$ but still beam sustained load capacity to about 80-90% of the ultimate load. Afterward shear cracks were severely widened and extended to compressive zone. Shear sliding of concrete pieces around shear crack could be clearly observed with bare eyes. This point is considered the ultimate capacity of beam in shear by a number of design codes, which the beam is in serious irreversible circumstances. According to this definition if numerical analysis is aiming to produce results for practical application such as RC member design, in average having $P_{Analysis} \approx 0.80\, P_{Exp.}$ can be considered as a quite satisfactory result.

6.2 Crack patterns

In order to investigate failure mechanism in RC beams, crack patterns in different load steps can explain behavior of the members and fracture process adequately. In other words good analysis should predict not only load capacity of the member with acceptable margin but also should be able to show other aspects of structure behavior such as deformation and crack development during loading process. Beam 14 is selected here for more detailed discussion. Figure 10 shows load-deflection response for two cases of conventional displacement control, Arc-length method and their evaluation by experiment. Both numerical results have quite good agreement with experiment. Displacement control method gave rise to divergence in solution

procedure a few steps after the peak though the results overly and peak load particularly are peak load vicinity have no numerical problem. It is however obvious to have such instability in certain steps if we look at the result obtained by means of Arc-length solution approach. Figure 10.2 depict load-displacement relationship for loading point with a snap-back at around $0.6P_u$ that foregoing method could successfully pass this point.

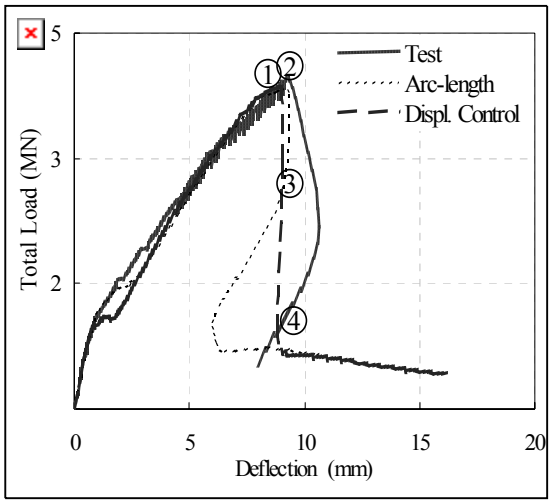

Figure 10-1. Beam 14 numerical and test results

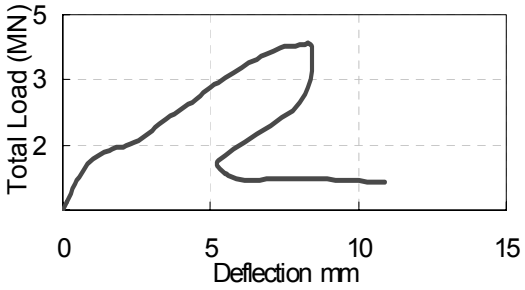

Figure 10-2. B14 response by arc-length method

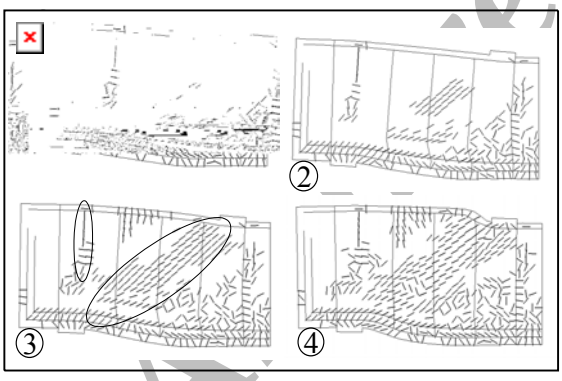

Figure 11.1. Analytical crack patterns of beam 14

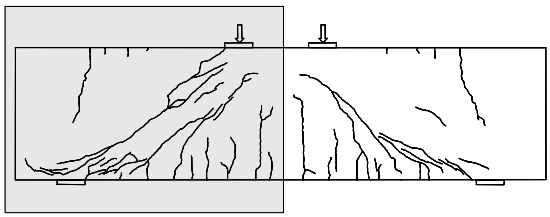

Figure 11.2. Experiment crack pattern of beam 14

Crack patterns obtained by analysis are shown in Figure 11.1 in four steps. Load steps indicated by 1 to 4 are peak load, just after the peak, first drop and consequent drop after the peak respectively. Experiment crack pattern of Figure 11.2 is in similar load level as number 3 pattern of Figure 11.1. As can be seen in these figures, crack formation and extension is well agreed with the experiment. It is noted however that crack due to the out of balance force in upper side of the beam above support is also adequately captured by analysis. The only noticeable difference between analysis and experiment in terms of crack prediction is

numerically observed cracks along longitudinal reinforcements. It is most possibly that the assumption of rigid bond between embedded steel bars and concrete elements caused such discrepancy between the results. Figure 11.1. 4 shows sliding between two parts of the beam due to the excessive shear deformation. This phenomenon is attributed to the loss of aggregate interlock, which is totally exhausted in this step.

7. CONCLUSIONS

To establish a platform for numerical evaluation of RC deep beams, sets of experiments have been carried out in three Japanese organizations of Public Works Research Institute and Kyushu Institute of Technology in a joint research basis with Hanshin Expressway Public Corporation. The primary objective of this study was to investigate RC underground structures subjected to vertical and lateral load. Due to the size and aspect ratio of each individual member of such structures which most of them are attributed to RC deep beam category, investigation on deep beams behavior was inevitable. In order to extend this study to a larger number of specimens, a finite element analysis is presented here and evaluated by aforementioned experimental evidences.

Beams are categorized in three categories based on a/d ratio. Beams with a/d>1 could successfully simulated by propose model. To analyze those beams a specialized finite element code is employed. The basic assumptions, which are adopted in FE analysis were smeared rotating crack model, fracture type constitutive model to eliminate mesh size effect with conventional displacement control as well as Arc-length nonlinear equation solution methods. The average ratio for analysis and experiment ultimate load was 0.86 that is in acceptable range with an adequate safety margin. If the results of FE analysis is to be used for real practice such as RC deep beam design work, the results will be in the range of the load (80% of the ultimate load) which is considered as maximum design load a member may carry. After this load however the beam will go to an irreversible state and sever damage with a possibility of sudden failure afterward. Therefore numerical results in this sense can satisfy safety of structures for design application. On the other hand beams with a/d<1 had analytical prediction (at least two out of three) higher than those observed in experiment. One possible reason out of others might be the theoretical assumption of rigid bond between steel reinforcement and concrete element. Such assumption gives rise to stiffer behavior, which observed clearly in those beams with extremely smaller deformation, and crack generation along longitudinal tensile reinforcement. Further works with rigorous theoretical basis are supposed to be carried out within the current project framework. Crack patterns observed in experiment and obtained through analysis have been another issues, which in good agreement obtained between two results.

Acknowledgements: Part of the experimental data used in this study was provided by Kyushu Institute of Technology and Hanshin Expressway Public Corporation. The authors

acknowledge great help of Professor Kenji Kosa and Dr. Tsutomu Nishioka from the above mentioned organizations.

REFERENCES

1. Salamy et al., A comparative study on RC deep beams behavior with shear span to depth ratio between 0.5 and 1.5, 8th Symposium on Ductility Design Method for Bridges, 2005.Feb.1-2, pp. 293-298, Tokyo, Japan.
2. Kotsovos Michael D., Behavior of reinforced concrete beams with a shear span to depth ratio between 1.0 and 2.5, *ACI Journal*, No.3, **81**(1984) 279-286.
3. Kwak Hyo-Gyoung and Flippou Flip C., Finite element analysis of reinforced concrete structures under monotonic loads, Report No. UCB/SEMM-90/14, Department of Civil Engineering, University of California Berkeley, November 1990, pp.32-35.
4. Hsu, Tomas T.C., *Unified Theory of Reinforced Concrete*, CRS Press Inc., 1993.
5. Japan Society of Civil Engineers, Standard specifications for concrete structures-2002, Structural performance verification. March 2002, Tokyo, Japan (in Japanese).
6. Feenstra, P.H., Computation aspects of biaxial stress in plain and reinforced concrete. PhD thesis, Delft University of Technology, 1993.
7. Hordijk, D.A., Local approach to fatigue of concrete. PhD thesis, Delft University of Technology, 1991.
8. Vecchio, Frank J. and Collins, Michael P., The Modified Compression-Field Theory for reinforced concrete elements subjected to shear, *ACI Journal*, No.2, **83**(1986) 219-231.